Theoretical Study of the Electronic Spectrum of the SiC^- Anion

Z.-L. Cai and J. P. François*

Department SBG, Institute for Materials Science (IMO), Universitaire Campus,
Limburgs Universitair Centrum, B-3590 Diepenbeek, Belgium

Received: July 28, 1998; In Final Form: December 2, 1998

The potential energy curves of the $X^2\Sigma^+$, $A^2\Pi$, and $B^2\Sigma^+$ states of the SiC^- anion and of the $X^3\Pi$ state of SiC have been calculated at the internally contracted multireference configuration interaction (CMRCI) level with Dunning's augmented correlation-consistent polarized valence quadruple-ζ (aug-cc-pVQZ) basis set. The equilibrium bond lengths (r_e), harmonic frequencies (ω_e), first-order anharmonicity constants ($\omega_e x_e$), rotational constants (B_e), dipole moments (μ_e), and dissociation (D_e) and excitation (T_e) energies for these states have been calculated. Core-correlation effects have been studied on both the $X^2\Sigma^+$ ground state and first excited $A^2\Pi$ state of SiC^-. The spectroscopic constants of the $A^2\Pi$ and $B^2\Sigma^+$ states of SiC^- and of the $X^3\Pi$ state of SiC are in good agreement with available experimental data. Adiabatic and vertical electron affinities (EA) of SiC($X^3\Pi$) have also been computed at the CMRCI/aug-cc-pVQZ level. The electronic transition moment functions (ETMFs) for both the $B^2\Sigma^+-X^2\Sigma^+$ and $B^2\Sigma^+-A^2\Pi$ transitions have been calculated at the CMRCI/aug-cc-pVQZ level. Based on both the calculated potential energy curves and the transition moments, the radiative lifetimes of the $B^2\Sigma^+(v'=0-10)$ states have been computed.

1. Introduction

Silicon−carbon species Si_xC_y are of interest in several scientific areas, such as material sciences and astrophysics. The simplest one of them, SiC, was identified by radioastronomy in dense interstellar clouds and stellar atmospheres,[1] and has been widely investigated experimentally and theoretically.[2−11] However, relatively little information is available on its negatively charged ion (anion), SiC^-. Recently, Grutter et al.[12] first identified SiC^- in solid neon matrixes (5 K) using mass-selected deposition. They measured the electronic absorption spectrum from the ground state ($X^2\Sigma^+$) to two excited states ($A^2\Pi$ and $B^2\Sigma^+$) of the SiC^- anion, with origin bands at 3538 and 21 683 cm^{-1}, respectively. The spectroscopic constants ω_e, $\omega_e x_e$, and T_e for the $A^2\Pi$ and $B^2\Sigma^+$ states were derived from their experiment.

The first theoretical study on SiC^- appeared in 1983, when Anglada et al.[13] studied low-lying electronic states of SiC^- and the electron affinity of SiC using the MRD-CI[14] (multireference single and double configuration interaction) method in conjunction with different basis sets (standard Huzinaga,[15] Dunning,[16] and Veillard[17] basis sets, plus bond functions, semidiffuse *d* functions and *s*, *p* Rydberg-like functions). Anglada et al. found only two doublet bound states ($X^2\Sigma^+$ and $A^2\Pi$) in contrast to the results for the isovalent C_2^-. In addition, they also predicted the spectroscopic constants r_e, ω_e, $\omega_e x_e$, B_e, α_e, T_e, and D_e for the $X^2\Sigma^+$ and $A^2\Pi$ states as well as the intensity for the $X^2\Sigma^+ \rightarrow A^2\Pi$ transition. In 1992, McLean et al.[10] computed spectroscopic constants for a series of diatomics including SiC and its negative ion, SiC^-, at the CISD and CISD+Q (singles and doubles configuration interaction with Davidson's quadruples correction[18]) levels using a large basis set (denoted here as MLC). McLean and co-workers only predicted ZPE (zero-point energy), $\Delta G_{1/2}$ (vibrational separation), and r_e of the excited $^2\Pi$ state of SiC^-. In 1994 in order to study vertical and adiabatic ionization energies and electron affinities of new Si_nC and Si_nO molecules, Boldyrev et al.[11] calculated r_e and ω_e of the $X^2\Sigma^+$ and $A^2\Pi$ states of SiC^- at the MP2(full)/6-311+G* level (second-order Møller−Plesset perturbation theory[19] correlating all electrons in conjunction with a polarized split-valence basis set[20−22]). They also predicted the excitation energy at the QCISD(T)/6-311G(2df) level (quadratic configuration interaction using single and double substitutions with a perturbative evaluation of the triple contribution[23] in conjunction with a split-valence basis set plus two *d*-types and one *f*-type polarized functions). They found that the $A^2\Pi$ state lies ∼3200 cm^{-1} above the $X^2\Sigma^+$ state, which is ∼200 cm^{-1} higher than the value computed by Anglada et al.[13] In 1996, Hunsicker and Jones[24] published a density functional theoretical study with simulated annealing on Si_xC_y and $Si_xC_y^-$ species with $x + y \leq 8$. In that paper, they predicted the bond length r_e of the $^2\Sigma^+$ ground state of SiC^- to be 3.17 bohr (1.677 Å).

It can be concluded from the preceding survey that no high-quality theoretical results for the spectroscopic constants of the SiC^- anion in the $X^2\Sigma^+$, $A^2\Pi$, and $B^2\Sigma^+$ states are available, and neither experimental nor theoretical data for the radiative lifetimes of the $B^2\Sigma^+(v')$ states have been published so far.

Recently, a lot of progress has been made in electron correlation methods such as multireference configuration interaction (MRCI),[25] internally contracted multireference configuration interaction (CMRCI),[26,27] and coupled cluster techniques (CCSD(T), a coupled cluster method with all single and double excitations supplemented with a quasiperturbative treatment for triple excitations[28−32]) in combination with basis sets of the atomic natural orbital[33,34] and correlation-consistent[35−37] families. These theoretical levels have made it possible to accurately predict spectroscopic constants for diatomic and polyatomic molecules with first and/or second-row atoms.[38,39] In our previous work on the $X^2\Sigma^+$ ground state and first excited $A^2\Pi$ state of SiN[40] and SiO^+,[41] we also found that core-correlation effects should be included in order to obtain a satisfactory accuracy.

In the present paper, we study the potential energy curves and electronic transition moment functions (ETMFs) of the SiC^-

10.1021/jp9831942 CCC: $18.00

anion by means of the CMRCI method with Dunning's correlation-consistent basis set family. We first present the spectroscopic constants r_e, ω_e, $\omega_e x_e$, B_e, μ_e, D_e, and T_e for the $X^2\Sigma^+$ ground state and first excited $A^2\Pi$ state of SiC^- at the CMRCI[26,27] level with Dunning's augmented correlation-consistent polarized valence double, triple and quadruple-ζ (aug-cc-pVDZ, aug-cc-pVTZ, and aug-cc-pVQZ) basis sets.[35-37] The basis set extension and core correlation are also investigated for both the $X^2\Sigma^+$ and $A^2\Pi$ states. The spectroscopic constants for the $B^2\Sigma^+$ state of SiC^- and the $X^3\Pi$ state of SiC will also be presented. The adiabatic and vertical electron affinities of $SiC(X^3\Pi)$ will be reported. For the $B^2\Sigma^+-X^2\Sigma^+$ and $B^2\Sigma^+-A^2\Pi$ transitions, we will focus our attention on the Franck-Condon region. Spontaneous emission probabilities for the $B^2\Sigma^+-X^2\Sigma^+$ and $B^2\Sigma^+-A^2\Pi$ transitions as well as the radiative lifetimes at different vibrational levels of the $B^2\Sigma^+(v'=0-10)$ states of the SiC^- anion are also reported. Our results will be compared with available experimental data.

2. Computational Details

The basis sets used in our calculations belong to Dunning's augmented correlation-consistent basis set family.[35-37] The aug-cc-pVDZ (augmented correlation-consistent polarized valence double-ζ) basis set is a [4s3p2d] general contraction of a (10s5p2d) primitive set for C, and a [5s4p2d] contraction of (13s9p2d) for Si. The aug-cc-pVTZ (augmented correlation-consistent polarized valence triple-ζ) basis set is a [5s4p3d2f] general contraction of a (11s6p3d2f) primitive set for C, and a [6s5p3d2f] contraction of (16s10p3d2f) for Si. Finally, the aug-cc-pVQZ (augmented correlation-consistent polarized valence quadruple-ζ) basis set is a (13s7p4d3f2g) primitive set contracted to [6s5p4d3f2g] for C, and (17s12p4d3f2g) contracted to [7s6p4d3f2g] for Si.

The CMRCI[26,27] and preliminary CASSCF[42,43] calculations were performed using the MOLPRO 96 program package.[44] Additional MP2(full)/6-311+G* calculations for both the $X^2\Sigma^+$ and $A^2\Pi$ states of the SiC^- anion were carried out using the Gaussian 94 program package.[45] Both quantum mechanical packages have been installed on IBM RS 6000 workstations at the Limburgs Universitair Centrum.

As a first step in the CMRCI calculations, the CASSCF approach was used in order to define the reference space. In separate calculations for the $X^2\Sigma^+$ and $A^2\Pi$ states of SiC^- and the $X^3\Pi$ state of SiC, the CASSCF wave functions were obtained individually for each state, while for the calculations of the $B^2\Sigma^+$ state of SiC^-, the SA-CASSCF (state averaged-complete active space self-consistent field[42,43]) approach was used. The active space for the CASSCF or SA-CASSCF calculations consists of all eight valence orbitals (i.e., the Si 3s, 3p orbitals and the C 2s,2p orbitals are active; 4 active orbitals in the σ space and 2 active orbitals in the $\pi_{x,y}$ space) leading to 9/8 CASSCF or SA-CASSCF calculations (9 electrons/8 orbitals) on SiC^- and to a 8/8 CASSCF calculation (8 electrons/8 orbitals) on SiC. The CMRCI(0.01) calculations include all single and double excitations from the subset of CASSCF or SA-CASSCF determinants that have coefficients of at least 0.01 in the CASSCF or SA-CASSCF wave functions. Davidson's correction[18] supplemented the CMRCI(0.01) calculations (denoted as CMRCI(0.01)+Q) in order to consider higher excitation effects; the CMRCI(0.01)+Q energies were used to depict the potential energy curves.

For the core-correlation calculations of the $X^2\Sigma^+$ and $A^2\Pi$ states of SiC^-, special basis sets were generated by first uncontracting the aug-cc-pVTZ basis set completely, then adding a single high-exponent ("hard") *p* function, and three "hard" *d* and two "hard" *f* functions. The exponents of the hard functions were obtained by successively multiplying the highest exponent of that particular angular momentum by a factor of 3 and rounding off to the nearest integer or half-integer. Such basis sets were found to recover essentially all effects of core-correlation for the first-row and second-row compounds.[40,41,46,47]

In our study, the CMRCI calculations have been carried out using the nondegenerate C_{2v} point group, a subgroup of $C_{\infty v}$ to which both SiC^- and SiC belong. In the C_{2v} point group, the Σ^+ state belongs to the A_1 representation, and Π to B_1 and B_2.

The vibrational calculations are performed using the VIBROT program from the MOLCAS 2 quantum chemistry software[48] providing the spectroscopic constants r_e, ω_e, $\omega_e x_e$, and B_e as well as the vibrational eigenfunctions. Since the values for the second-order anharmonicity constants ($\omega_e y_e$) were found to be very small and subjected to large error bars, their values have not been included in the present paper. The dipole moments μ_e for each electronic state have been recalculated at the equilibrium bond distance r_e. Since the CMRCI method is not size-consistent, the dissociation energies (D_e) for the electronic states have been computed by the supermolecular approach ($r = 100$ a_0), which yields more accurate bond energies than summing the respective atomic energies at the dissociation limit.[49]

In the present work, the Einstein $A_{v'v''}$ coefficients (in s^{-1}) are computed using the following expression[50]

$$A_{v'v''} = 2.026 \times 10^{-6} g \bar{\nu}^3_{v'v''} |D_{v'v''}|^2 \qquad (1)$$

where $\bar{\nu}_{v'v''}$ is the transition energy (in cm^{-1}) between v' of the upper state and v'' of the lower state, $D_{v'v''}$ is the electronic transition moment between the v' and v'' levels, and g is a statistical weighting factor

$$g = (2 - \delta_{0,\lambda'+\lambda''})/(2 - \delta_{0,\lambda'}) \qquad (2)$$

where λ'' and λ' denote the orbital angular moments of the upper and lower states.

The $D_{v'v''}$ values are computed numerically using a spline representation of the CMRCI(0.01)+Q/aug-cc-pVQZ potential and transition moments. Rotationless potentials are used throughout. It should further be remarked that the influence of vibration-rotation interactions on the lifetime is rather small. The radiative lifetime ($\tau_{v'}$) of a vibrational level depends on the sum of the transition probabilities to all lower vibrational levels in all lower electronic states. If rotational effects are neglected, the lifetime can be simply computed as

$$\tau_{v'} = (\sum_{v''} A_{v'v''})^{-1} \qquad (3)$$

3. Results and Discussion

3.1. Atomic Asymptotes. As a first step in ascertaining the accuracy of both the electron correlation method and basis sets used in the calculations, the atomic splitting for $Si^-(^2D_u-^4S_u)$ was calculated at the CMRCI(0.01) and CMRCI(0.01)+Q levels since $SiC^-(X^2\Sigma^+,A^2\Pi)$ correlate to the dissociation channel $Si^-(^4S_u) + C(^3P_g)$ and $SiC^-(B^2\Sigma^+)$ to $Si^-(^2D_u) + C(^3P_g)$. The calculated values of the atomic splitting are CMRCI(0.01)/aug-cc-pVDZ 9116 cm^{-1}, aug-cc-pVTZ 7888 cm^{-1}, and aug-cc-pVQZ 7660 cm^{-1}; CMRCI(0.01)+Q/aug-cc-pVDZ 8620 cm^{-1}, aug-cc-pVTZ 7266 cm^{-1}, and aug-cc-pVQZ 7027 cm^{-1}. The experimental value[51] is 6952 cm^{-1}. The results with the aug-cc-pVDZ, aug-cc-pVTZ, and aug-cc-pVQZ basis sets can be extrapolated to the basis set limit (aug-cc-pV∞Z) using the three-

TABLE 1: Spectroscopic Constants of the $X^2\Sigma^+$, $A^2\Pi$, and $B^2\Sigma^+$ States of SiC$^-$ and the $X^3\Pi$ State of SiC[a]

level	r_e	ω_e	$\omega_e x_e$	B_e	μ_e	D_e	T_e
$X^2\Sigma^+$							
CMRCI(0.01)+Q/aug-cc-pVDZ	1.7286	949.6	6.21	0.67181			
CMRCI(0.01)+Q/aug-cc-pVTZ	1.7051	985.5	6.10	0.69045			
CMRCI(0.01)+Q/aug-cc-pVQZ	1.6950	1001.2	6.06	0.69872	1.48	5.29	
CMRCI(0.01)+Q/aug-cc-pV∞Z estimate	1.6874	1013.4		0.70532			
CMRCI(0.01)+Q/aug-cc-pVTZ(uncontracted)	1.7039	986.3	6.12	0.69137			
CMRCI(0.01)+Q/no core	1.6940	993.8	6.13	0.69948			
CMRCI(0.01)+Q/core1	1.6865	1005.3	6.07	0.70578			
CMRCI(0.01)+Q/core2	1.6860	1006.7	6.06	0.70621			
CMRCI+Q/best estimate	1.6794	1026.3		0.71205			
MRD-CI[b]	1.70	976	4.5	0.693			
MP2(full)/6-311+G*[c]	1.759	1127					
DFT/plane waves[d]	1.677						
$A^2\Pi$							
CMRCI(0.01)+Q/aug-cc-pVDZ	1.7909	882.1	5.61	0.62587			3075.8
CMRCI(0.01)+Q/aug-cc-pVTZ	1.7692	913.1	5.29	0.64128			3189.0
CMRCI(0.01)+Q/aug-cc-pVQZ	1.7599	925.9	5.26	0.64809	2.90	4.89	3228.9
CMRCI(0.01)+Q/aug-cc-p-V∞Z estimate	1.7529	934.9		0.65348			3256.9
CMRCI(0.01)+Q/aug-cc-pVTZ(uncontracted)	1.7682	913.1	5.34	0.64201			3189.3
CMRCI(0.01)+Q/no core	1.7586	918.9	5.24	0.64906			3247.6
CMRCI(0.01)+Q/core1	1.7510	928.7	4.77	0.65472			3440.4
CMRCI(0.01)+Q/core2	1.7506	929.7	4.71	0.65505			3465.3
CMRCI+Q/best estimate	1.7449	945.7		0.65947			3474.6
MRD-CI[b]	1.77	949	5.5	0.642			∼3000
CISD/MLC[e]	1.736	1033.1[f]					
CISD+Q/MLC[e]	1.749	997.6[f]					
MP2(full)/6-311+G*[c]	1.710	951					
QCISD/6-311+G(2df)[c]							∼3200
MP2(full)/6-311+G* (this work)	1.7548	998					∼3000
expt (in neon)[g]		941 ± 3	6 ± 1				3556 ± 2
$B^2\Sigma^+$							
CMRCI(0.01)+Q/aug-cc-pVQZ	1.7858	693.5	4.66	0.62929	1.35	3.50	21278.5
expt (in neon)[g]		717 ± 25					21813 ± 20
SiC ($X^3\Pi$)							
CMRCI(0.01)+Q/aug-cc-pVQZ	1.7316	950.6	5.87	0.66948	1.48	4.31	
MRD-CI[h]	1.75	960					
QCISD(T)/MC-311G(2df)[i]	1.724	978.7	6.24	0.67502		4.13	
CISD/MLC[j]	1.704	1027.4[k]					
CISD+Q/MLC[j]	1.721	990.3[k]					
MP2(full)/6-311+G*[c]	1.702	896					
expt	1.722[l]	964.6[m] 965.16(24)[n]	5.6[m] 5.910(36)[n]				

[a] r_e is expressed in Å, μ_e in debye, all the other constants in cm^{-1}. [b] Reference 13. [c] Reference 11. [d] Reference 24. [e] Reference 10. [f] Vibrational separation $\Delta G_{1/2} = \omega_e - 2\omega_e x_e + 13/4\ \omega_e y_e$. [g] Reference 12. [h] Reference 7. [i] Reference 8. [j] Reference 10. [k] Vibrational averaged $\omega_0 = \omega_e - \omega_e x_e + 3/4\ \omega_e y_e$. [l] Reference 3. [m] Reference 4. [n] Reference 5.

point extrapolation technique (Schwartz6(2,3,4)) by Martin[52] for energies; the exponential formula proposed by Woon and Dunning[53] has been used for other spectroscopic constants. The CMRCI(0.01)/aug-cc-pV∞Z value of 7543 cm^{-1} is 591 cm^{-1} too high, while the CMRCI(0.01)+Q/aug-cc-pV∞Z result (6909 cm^{-1}) is only 43 cm^{-1} too low with respect to experiment. It can be concluded that the CMRCI+Q method predicts more accurate results for energy differences (excitation energies) among different electronic states because it can also consider higher excitation effects besides single and double ones.

3.2. Spectroscopic Constants of the $X^2\Sigma^+$ and $A^2\Pi$ States of SiC$^-$.

3.2.1. The $X^2\Sigma^+$ State. Our spectroscopic constants r_e, ω_e, $\omega_e x_e$, B_e, μ_e, and D_e for the $X^2\Sigma^+$ ground state of SiC$^-$ are shown in Table 1; previous theoretical results are also listed in Table 1 for comparison. The r_e value of 1.70 Å at the MRD-CI level by Anglada et al.[13] is 0.059 Å shorter than the value calculated at the MP2(full)/6-311+G* level by Boldyrev et al.[11] There is also a large discrepancy for ω_e between the MRD-CI and MP2(full)/6-311+G* levels (151 cm^{-1}). Because there are no experimental data available for comparison, it is not clear which theoretical level is the most accurate one.

In order to improve the previous theoretical results, we first perform calculations at the CMRCI(0.01)+Q/aug-cc-pVDZ to aug-cc-pVQZ levels. We extend the basis set from aug-cc-pVDZ to aug-cc-pVQZ up to the limit (aug-cc-pV∞Z) using the exponential formula proposed by Woon and Dunning[53] for extrapolating r_e, ω_e, and B_e. It is seen that r_e decreases and ω_e increases when the basis set is expanded from aug-cc-pVDZ to aug-cc-pV∞Z. The r_e and ω_e values at the MRCI(0.01)+Q level when the basis set limit is reached are 1.6874 Å and 1013.4 cm^{-1}, respectively. Since we have found previously for SiN[40] and SiO$^+$ [41] that core correlation should be included in order to obtain accurate spectroscopic constants for both species, isovalent with SiC$^-$ and since there are no experimental data available for the $X^2\Sigma^+$ ground state of SiC$^-$, it is essential to include core correlation in the calculations for the anion.

Core-correlation calculations require special basis sets, which have been described in the Computational Details section. The spectroscopic constants were first calculated at the CMRCI(0.01)+Q level with the aug-cc-pVTZ (uncontracted) basis set. The results are very close to those with the aug-cc-pVTZ basis set, indicating that the contraction error is not overly important.

After adding hard *p*, *d*, and *f* functions to aug-cc-pVTZ (uncontracted), only valence electrons (i.e., the 1s, 2s, and 2p electrons of Si and 1s electrons of C have been excluded) have been considered first; the results are denoted as CMRCI-(0.01)+Q/no core. The r_e value at the CMRCI(0.01)+Q/no core level is now 1.6940 Å, being 0.0099 Å shorter than the corresponding aug-cc-pVTZ(uncontracted) one. The ω_e value at the CMRCI(0.01)+Q/no core level increases by 7.5 cm^{-1} with respect to the corresponding aug-cc-pVTZ(uncontracted) one. All the electrons, except the 1s electrons of Si, are correlated now and the theoretical level is denoted as CMRCI-(0.01)+Q/core1. At that level, r_e decreases by 0.0075 Å, ω_e increases by 11.5 cm^{-1}, and $\omega_e x_e$ decreases by 0.06 cm^{-1} compared to the no core values. We have also correlated the 1s electrons of Si in the calculations (denoted as core2) in order to identify the 1s orbital effect of Si. At the CMRCI(0.01)+Q/core2 level, r_e decreases by 0.0005 Å, ω_e increases by only 1.4 cm^{-1}, and $\omega_e x_e$ decreases by only 0.01 cm^{-1}. It can thus be concluded that the 1s electrons of Si can be safely neglected in our core-correlation calculations.

The effects of core correlation by the inclusion of the 1s, 2s, and 2p electrons of Si and 1s electrons of C are considered now as additive corrections to the CMRCI(0.01)+Q/aug-cc-pV∞Z values, yielding the values marked "best estimate" for the $X^2\Sigma^+$ state at the CMRCI(0.01)+Q level in Table 1. The best estimate r_e and ω_e values are 1.6794 Å and 1026.3 cm^{-1}, respectively. In our previous work on SiO$^+$,[41] we have found that the CASSCF method predicts less accurate spectroscopic constants than the CMRCI(0.01) and CMRCI(0.01)+Q methods. Hence, we believe that our best estimate at the CMRCI(0.01)+Q level should provide accurate spectroscopic constants for the $X^2\Sigma^+$ state of SiC$^-$. It should also be remarked that the r_e value computed using density functional theory (DFT) by Hunsicker and Jones[24] is in good agreement with our "best estimate".

3.2.2. The A²Π State. The calculated spectroscopic constants of the $A^2\Pi$ state of SiC$^-$ are collected in Table 1. Previous theoretical and recent experimental data are also listed for comparison.

The ω_e values at the MRD-CI[13] and MP2(full)/6-311+G* [11] levels are close to the recent experimental one of 941 ± 3 cm^{-1}.[12] The excitation energies at the MRD-CI[13] and QCISD/6-311+G(2df)[11] levels are both smaller than the recent experimental result of 3556 ± 2 cm^{-1}.[12] There are large discrepancies for r_e among different electron correlation methods. It should be noted that the MP2 value of 1.710 Å is too short. We have also performed MP2(full)/6-311+G* calculations on both the $X^2\Sigma^+$ and $A^2\Pi$ states using the Gaussian 94 program package and obtained the same results as Boldyrev et al.[11] for the $X^2\Sigma^+$ state. However, for the $A^2\Pi$ state, we obtain very different values for r_e and ω_e (1.7548 Å and 998 cm^{-1}, respectively). Our MP2(full)/6-311+G* T_e value of ~3000 cm^{-1} is close to the previous MRD-CI one. Apparently there are some doubts on the previous MP2(full)/6-311+G* results for the $A^2\Pi$ state.

The ω_e value at the CMRCI(0.01)+Q/aug-cc-pV∞Z level is only ca. 6 cm^{-1} smaller than experiment. The CMRCI(0.01)+Q/aug-cc-pV∞Z T_e value of 3256.9 cm^{-1} is 299 cm^{-1} smaller than experiment.

We have also carried out no core and core calculations at the CMRCI(0.01)+Q level for the $A^2\Pi$ state as we did for the $X^2\Sigma^+$ ground state, and made the same basis set extension beyond aug-cc-pVTZ and the same additivity assumption for the inclusion of core correlation. In doing so we obtained the best estimate spectroscopic constants at the CMRCI(0.01)+Q level. The best estimate ω_e value at the CMRCI(0.01)+Q level (945.7 cm^{-1}) is very close to the experimental result of 941 ± 3 cm^{-1}. It should be noted that our best estimate T_e value at the CMRCI(0.01)+Q level is only ca. 80 cm^{-1} lower than the experimental one of 3556 ± 2 cm^{-1}.

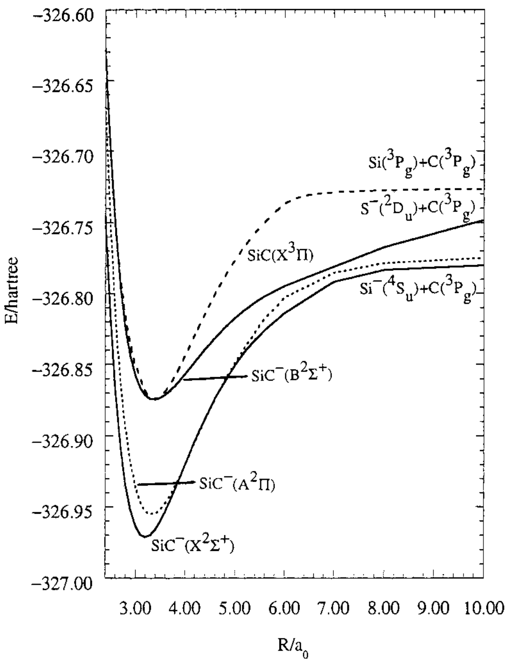

Figure 1. CMRCI(0.01)+Q/aug-cc-pVQZ potential energy curves for the $X^2\Sigma^+$, $A^2\Pi$, and $B^2\Sigma^+$ states of SiC$^-$ and for the $X^3\Pi$ state of SiC.

3.3. Spectroscopic Constants of the B²Σ⁺ State of SiC⁻ and the X³Π State of SiC. The calculated potential energy curves for the $X^2\Sigma^+$, $A^2\Pi$, and $B^2\Sigma^+$ states of SiC$^-$ and for the $X^3\Pi$ ground state of SiC at the CMRCI(0.01)+Q/aug-cc-pVQZ level are depicted in Figure 1. It is seen that the $X^2\Sigma^+$, $A^2\Pi$, and $B^2\Sigma^+$ electronic states of the SiC$^-$ anion all lie below the $X^3\Pi$ ground state of the neutral species.

At the CMRCI(0.01)/aug-cc-pVQZ level, our calculated adiabatic (vertical) electron affinities (EAs) of SiC($X^3\Pi$) (SiC($X^3\Pi$) + e^- → SiC$^-$($X^2\Sigma^+$) or SiC$^-$($A^2\Pi$)) are 2.67(2.65) or 2.27(2.25) eV. There are no accurate experimental data for comparison so far; however, some theoretical studies on adiabatic and vertical EAs have been published and the calculated values differ depending on the theoretical levels. In 1983, Anglada et al.[13] reported a value of 1.98 eV for the vertical EA of SiC (SiC($X^3\Pi$) + e^- → SiC$^-$($X^2\Sigma^+$)) from an ab initio MRD-CI calculation. In 1994, Boldyrev et al.[11] obtained a value of 2.25 eV for the first adiabatic EA of SiC, which differs slightly from their vertical EA value of 2.32 eV. In 1996, Hunsicker and Jones[24] also predicted the vertical EA to be 2.55 eV (SiC($X^3\Pi$) + e^- → SiC$^-$($X^2\Sigma^+$)) in their density functional theoretical study. It is obvious that our adiabatic (vertical) EA values are somewhat higher than the previous theoretical ones.

The calculated spectroscopic constants of the SiC$^-$($B^2\Sigma^+$) and SiC($X^3\Pi$) states are shown in Table 1.

For the SiC$^-$($B^2\Sigma^+$) state, our ω_e value of 693.5 cm^{-1} is close to the recent experimental one of 717 ± 25 cm^{-1}, the excitation energy T_e value of 21 278.5 cm^{-1} is only about 500 cm^{-1} smaller than the experimental one of 21 813 ± 20 cm^{-1} from electronic absorption spectra of SiC$^-$ in neon matrixes.

The SiC($X^3\Pi$) state has been widely investigated both experimentally and theoretically. Some data are listed in Table 1 for comparison. Our values for the spectroscopic constants r_e, ω_e, $\omega_e x_e$, and B_e are very close to the available experimental

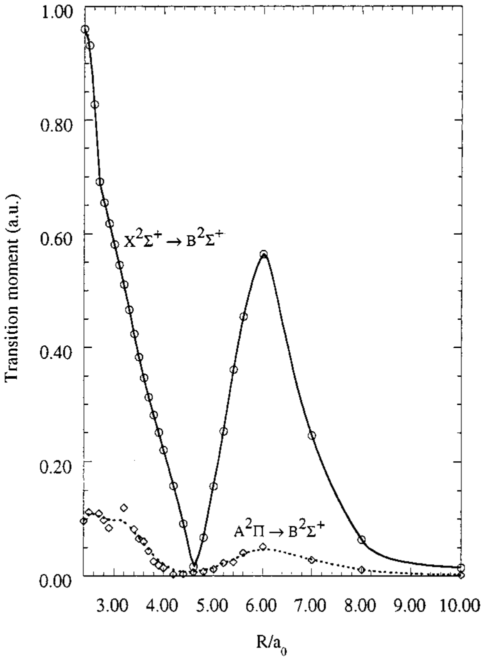

Figure 2. Transition moment curves for the $B^2\Sigma^+-X^2\Sigma^+$ and $B^2\Sigma^+-A^2\Pi$ transitions of SiC$^-$.

data. It is noted that the present CMRCI(0.01)+Q/aug-cc-pVQZ results are also similar to the previous best theoretical ones by Martin et al.[8] Since the spectroscopic constants for SiC$^-$($B^2\Sigma^+$) and SiC($X^3\Pi$) are in very good agreement with the experimental data, it may be concluded that our calculated adiabatic (vertical) EAs of SiC should also be reliable, although there have been no accurate experimental values available so far allowing direct comparison.

3.4. Electronic Transition Moment Functions of the $B^2\Sigma^+-X^2\Sigma^+$ and $B^2\Sigma^+-A^2\Pi$ Transitions. ***3.4.1. $B^2\Sigma^+-X^2\Sigma^+$.*** As has been mentioned in the Introduction, we limit our discussion to the Franck−Condon region, which is the most important one from the experimental point of view.

The $B^2\Sigma^+-X^2\Sigma^+$ electronic transition moment function (ETMF) is shown in Figure 2. At short internuclear distances, the ETMF decreases very rapidly with increasing R, reaching its minimum value of 0.02 au at 4.60 a_0. From 4.61 to 6.00 a_0, the ETMF increases almost linearly up to 6.00 a_0, where it reaches a value of 0.57 au, and then decreases smoothly toward zero at the asymptotic limit. It should be remarked that at large internuclear separations, the ETMF must be zero since it is associated with the forbidden Si$^-$(^2D_u)−Si$^-$(^4S_u) atomic transition.

The shape of the ETMF between $2.40 \leq R \leq 4.60$ a_0 can be expressed well by a fourth-order polynomial (in au):

$$R_e(R) = 14.138 - 13.505R + 5.1518R^2 - 0.89212R^3 + 0.057691R^4 \quad (4)$$

The behavior of $R_e(R)$ may be rationalized by considering the configurations of both the $X^2\Sigma^+$ and $B^2\Sigma^+$ states. Between 2.40 and 4.60 a_0, the $X^2\Sigma^+$ state is dominated mainly by the following two configurations: (I) $5\sigma^2 6\sigma^2 7\sigma^1 2\pi^4$ and (II)$5\sigma^2 6\sigma^2 7\sigma^1 2\pi^2 3\pi^2$, always with configuration I being the most important one. The $B^2\Sigma^+$ state is mainly described by configurations III and IV: (III) $5\sigma^2 6\sigma^1 7\sigma^2 2\pi^4$ and (IV) $5\sigma^2 6\sigma^2 7\sigma^1 2\pi^3 3\pi^1$, both configurations being the important ones when $R \leq 3.20$ a_0, and beyond 3.20 a_0, configuration (IV) is the most important one.

Therefore, in the Franck−Condon region during the $B^2\Sigma^+-X^2\Sigma^+$ transition, the electron is essentially transferred from the 6σ to the 7σ orbital and from the 2π to the 3π orbital. The 6σ orbital is primarily associated with the Si atom and the 7σ molecular orbital exhibits a contribution from either Si or C, but the C contribution increases with increasing internuclear distance and has around 4.60 a_0 a major contribution from the C 2p orbital. The 2π orbital has a contribution from either Si or C, but the Si contribution increases as R increases; the 3π orbital has always a major contribution from the C atom. Hence, the electron overlap integral between the two orbitals, centered on different atoms, should be affected by the internuclear distance, and decreases as the internuclear distance increases, which explains the behavior of the ETMF of the $B^2\Sigma^+-X^2\Sigma^+$ transition in the Franck−Condon region.

3.4.2. $B^2\Sigma^+-A^2\Pi$. The $B^2\Sigma^+-A^2\Pi$ ETMF is also shown in Figure 2 and we limit also our discussion to the Franck−Condon region, as we did for the $B^2\Sigma^+-X^2\Sigma^+$ transition.

The ETMF of the $B^2\Sigma^+-A^2\Pi$ transition is much smaller than that of the $B^2\Sigma^+-X^2\Sigma^+$ transition; however, it has a similar shape as that of the $B^2\Sigma^+-X^2\Sigma^+$ one in the entire region.

Similar to the $B^2\Sigma^+-X^2\Sigma^+$ transition, the shape of the ETMF between $2.40 \leq R \leq 4.60$ a_0 (Franck−Condon region) can also be expressed by a fourth-order polynomial (in au):

$$R_e(R) = 15.916 - 19.967R + 9.3492R^2 - 1.9202R^3 + 0.14557R^4 \quad (5)$$

We analyze the configuration nature of the $B^2\Sigma^+$ and $A^2\Pi$ states between 2.40 and 4.60 a_0 as above. The $A^2\Pi$ state is always dominated by the single configuration (V) $5\sigma^2 6\sigma^2 7\sigma^2 2\pi^3$.

Therefore, in the Franck−Condon region during the $B^2\Sigma^+-A^2\Pi$ transition, the electron transfer is essentially from the 6σ to the 2π orbital and from the 7σ to the 3π orbital. As we discussed above, both the 2π and 3π orbitals have contributions from either Si or C. Although the contributions from the Si atom on the 2π orbital and from the C atom on the 3π orbital increase with increasing internuclear distance, the electron overlap integral between these orbitals, centered on different atoms, should also be affected by the internuclear distances, and decreases as the internuclear increases. This explains again the behavior of the ETMF of the $B^2\Sigma^+-A^2\Pi$ transition in the Franck−Condon region.

3.5. Radiative Lifetimes of the $B^2\Sigma^+(v')$ States of SiC$^-$. Since we obtained the ETMFs for the $B^2\Sigma^+-X^2\Sigma^+$ and $B^2\Sigma^+-A^2\Pi$ transitions and analyzed the ETMF behavior in the Franck−Condon region, we also calculated the transition moment matrix elements $\langle v'|R_e|v''\rangle$ between the $B^2\Sigma^+(v')$ and $X^2\Sigma^+(v'')$ states and between the $B^2\Sigma^+(v')$ and $A^2\Pi$ (v'') states of SiC$^-$, as well as spontaneous emission probabilities $A_{v',v''}$ for these two transitions. The spontaneous emission probabilities for the $B^2\Sigma^+(v')-X^2\Sigma^+(v'')$ and $B^2\Sigma^+(v')-A^2\Pi(v'')$ transitions are presented in Tables 2 and 3, respectively. The radiative lifetimes at different vibrational levels ($v' = 0-10$) of the $B^2\Sigma^+$ state to the $X^2\Sigma^+$ and $A^2\Pi$ states are derived from the spontaneous emission probabilities $A_{v',v''}$ and are collected in Table 4. There are no experimental data available for comparison. In our previous work on the $B^2\Sigma^+(v')-X^2\Sigma^+(v'')$ transition of SiO$^+$,[54] we have found that the CMRCI method in conjunction with the Dunning's cc-pVQZ basis set can predict accurate radiative lifetimes, being in very good agreement with experimental data. Since the SiC$^-$ anion is isovalent with SiO$^+$, we believe that our radiative lifetimes of the SiC$^-$ anion are reliable.

TABLE 2: Calculated Spontaneous Emission Probabilities $A_{v',v''}$ for the $B^2\Sigma^+(v') \rightarrow X^2\Sigma^+(v'')$ Transition of SiC^-[a]

v''/v'	0	1	2	3	4	5	6	7	8	9	10
0	0.001 706	0.001 976	0.001 185	0.000 480	0.000 146	0.000 035	0.000 007	0.000 001	0.000 000	0.000 000	0.000 000
1	0.001 079	0.000 004	0.000 933	0.001 491	0.001 072	0.000 503	0.000 175	0.000 048	0.000 010	0.000 002	0.000 000
2	0.000 370	0.000 507	0.000 301	0.000 110	0.000 964	0.001 300	0.000 929	0.000 454	0.000 168	0.000 049	0.000 012
3	0.000 090	0.000 468	0.000 058	0.000 482	0.000 039	0.000 307	0.001 027	0.001 163	0.000 796	0.000 393	0.000 151
4	0.000 017	0.000 196	0.000 311	0.000 023	0.000 301	0.000 260	0.000 009	0.000 508	0.001 047	0.001 033	0.000 680
5	0.000 002	0.000 054	0.000 242	0.000 108	0.000 152	0.000 070	0.000 343	0.000 073	0.000 109	0.000 661	0.001 019
6	0.000 000	0.000 011	0.000 097	0.000 205	0.000 006	0.000 209	0.000 001	0.000 225	0.000 231	0.000 002	0.000 249
7	0.000 000	0.000 001	0.000 026	0.000 126	0.000 119	0.000 018	0.000 148	0.000 067	0.000 064	0.000 268	0.000 102
8	0.000 000	0.000 000	0.000 005	0.000 045	0.000 127	0.000 040	0.000 073	0.000 052	0.000 137	0.000 000	0.000 168
9	0.000 000	0.000 000	0.000 001	0.000 010	0.000 062	0.000 100	0.000 002	0.000 102	0.000 002	0.000 131	0.000 039
10	0.000 000	0.000 000	0.000 000	0.000 002	0.000 018	0.000 071	0.000 058	0.000 008	0.000 083	0.000 014	0.000 069

[a] In ns^{-1}.

TABLE 3: Calculated Spontaneous Emission Probabilities $A_{v',v''}$ for the $B^2\Sigma^+(v') \rightarrow A^2\Pi(v'')$ Transition of SiC^-[a]

v''/v'	0	1	2	3	4	5	6	7	8	9	10
0	0.000 102	0.000 027	0.000 001	0.000 002	0.000 003	0.000 001	0.000 000	0.000 001	0.000 001	0.000 000	0.000 000
1	0.000 000	0.000 063	0.000 025	0.000 000	0.000 003	0.000 004	0.000 001	0.000 000	0.000 001	0.000 001	0.000 001
2	0.000 000	0.000 004	0.000 031	0.000 025	0.000 000	0.000 003	0.000 004	0.000 001	0.000 000	0.000 001	0.000 002
3	0.000 001	0.000 000	0.000 006	0.000 013	0.000 026	0.000 003	0.000 002	0.000 003	0.000 001	0.000 000	0.000 001
4	0.000 000	0.000 001	0.000 000	0.000 006	0.000 005	0.000 025	0.000 008	0.000 000	0.000 003	0.000 001	0.000 000
5	0.000 000	0.000 000	0.000 000	0.000 000	0.000 004	0.000 002	0.000 022	0.000 014	0.000 000	0.000 002	0.000 002
6	0.000 000	0.000 000	0.000 000	0.000 000	0.000 000	0.000 003	0.000 000	0.000 016	0.000 018	0.000 003	0.000 001
7	0.000 000	0.000 000	0.000 000	0.000 000	0.000 000	0.000 000	0.000 001	0.000 000	0.000 010	0.000 019	0.000 007
8	0.000 000	0.000 000	0.000 000	0.000 000	0.000 000	0.000 000	0.000 000	0.000 001	0.000 000	0.000 006	0.000 017
9	0.000 000	0.000 000	0.000 000	0.000 000	0.000 000	0.000 000	0.000 000	0.000 000	0.000 000	0.000 000	0.000 003
10	0.000 000	0.000 000	0.000 000	0.000 000	0.000 000	0.000 000	0.000 000	0.000 000	0.000 000	0.000 000	0.000 000

[a] In ns^{-1}.

TABLE 4: Lifetimes (in ns) of the $B^2\Sigma^+(v')$ States and the Contributions to These Lifetimes from the $X^2\Sigma^+$ and $A^2\Pi$ States of the SiC^- Anion

	contribution		
v'	total lifetime	$X^2\Sigma^+$	$A^2\Pi$
0	297.04	306.43	9 691.53
1	301.78	310.69	10 518.44
2	310.42	316.72	15 614.24
3	319.48	324.36	21 236.60
4	327.54	332.22	23 272.44
5	334.83	339.56	24 041.83
6	341.90	346.57	25 383.83
7	349.02	353.58	27 045.39
8	356.38	360.94	28 197.29
9	364.10	368.74	28 953.29
10	372.10	376.78	29 946.46

4. Conclusions

The potential energy curves of the $X^2\Sigma^+$, $A^2\Pi$, and $B^2\Sigma^+$ states of the SiC^- anion and of the $X^3\Pi$ state of SiC have been calculated at the CMRCI(0.01)+Q/aug-cc-pVQZ level. The spectroscopic constants r_e, ω_e, $\omega_e x_e$, B_e, μ_e, D_e, and T_e for the electronic states of SiC^- and for the ground state of SiC are obtained. Core-correlation effects have also been studied for both the $X^2\Sigma^+$ ground state and the first excited $A^2\Pi$ state of SiC^-. Very accurate spectroscopic constants, being in very good agreement with the available experimental data, have been obtained for both states. The spectroscopic constants of the $B^2\Sigma^+$ state of the SiC^- anion and of the $X^3\Pi$ state of SiC are also in good agreement with available experimental data. Our adiabatic (vertical) electron affinities of $SiC(X^3\Pi)$, calculated at the CMRCI level, are somewhat higher than previous theoretical ones. The ETMFs of the $B^2\Sigma^+-X^2\Sigma^+$ and $B^2\Sigma^+-A^2\Pi$ transitions have been calculated at the CMRCI(0.01)/aug-cc-pVQZ level. The ETMFs for both transitions have a strong R dependence in the $2.40 \leq R \leq 4.60$ a_0 region and can be described by fourth-order polynomial. Radiative lifetimes at 11 vibrational levels of the $B^2\Sigma^+(v')$ state have been obtained.

Acknowledgment. Z.L.C. acknowledges a fellowship as a Visiting Professor from the Limburgs Universitair Centrum (LUC). Financial support from the "Bijzonder Onderzoeksfonds" (BOF) of the LUC is also gratefully acknowledged.

References and Notes

(1) Cernicharo, J.; Gottlieb, C. A.; Guélin, M.; Thaddeus, P.; Vrtilek, J. M. *Astrophys. J. Lett.* **1989**, *341*, L25.

(2) Bernath, P. F.; Rogers, S. A.; O'Brien, L. C.; Brazier, C. R.; McLean, A. D. *Phys. Rev. Lett.* **1988**, *60*, 197.

(3) Brazier, C. R.; O'Brien, L. C.; Bernath, P. F. *J. Chem. Phys.* **1989**, *91*, 7384.

(4) Ebben, M.; Drabbels, M.; ter Meulen, J. J. *J. Chem. Phys.* **1991**, *95*, 2292.

(5) Butenhoff, J. T.; Rohlfing, E. A. *J. Chem. Phys.* **1991**, *95*, 3939.

(6) Sefyani, F. L.; Schamps, J. *Astrophys. J.* **1994**, *434*, 816.

(7) Bruna, P. J.; Peyerimhoff, S. D.; Buenker, R. J. *J. Chem. Phys.* **1980**, *72*, 5437.

(8) Martin, J. M. L.; François, J. P.; Gijbels, R. *J. Chem. Phys.* **1990**, *92*, 6655.

(9) Langhoff S. R.; Bauschlicher, Jr. C. W. *J. Chem. Phys.* **1992**, *93*, 42.

(10) McLean, A. D.; Liu, B.; Chandler, G. S. *J. Chem. Phys.* **1992**, *97*, 8459.

(11) Boldyrev, A. I.; Simons, J.; Zakrzewski, V. G.; von Niessen, W. *J. Phys. Chem.* **1994**, *98*, 1427.

(12) Grutter, M.; Freivogel, P.; Maier, J. P. *J. Phys. Chem.* **1997**, *101*, 275.

(13) Anglada, J.; Bruna, P. J.; Peyerimhoff, S. D.; Buenker, R. J. *J. Phys. B. At. Mol. Phys.* **1983**, *16*, 2649.

(14) Buenker, R. J.; Peyerimhoff, S. D.; Butscher, W. *Mol. Phys.* **1978**, *35*, 771, and references therein.

(15) Huzinaga, S. *J. Chem. Phys.* **1965**, *42*, 1293.

(16) Dunning, Jr., T. H. *J. Chem. Phys.* **1970**, *53*, 2823.

(17) Veillard, A. *Theor. Chim. Acta* **1968**, *12*, 405.

(18) Langhoff S. R.; Davidson, E. R. *Int. J. Quantum Chem.* **1974**, *8*, 61.

(19) Møller C.; Plesset, M. J. *Phys. Rev.* **1934**, *46*, 618.

(20) (a) Frisch, M. J.; Pople, J. A.; Binkley, J. S. *J. Chem. Phys.* **1984**, *80*, 3265. (b) Krishnan, R.; Binkley, J. S.; Seeger, R.; Pople, J. A. *J. Chem. Phys.* **1980**, *72*, 650.

(21) Clark, T.; Chandrasekhar, J.; Spitznagel, G. W.; Schleyer, P.v. R. *J. Comput. Chem.* **1983**, *4*, 294.

(22) McLean A. D.; Chandler, G. S. *J. Chem. Phys.* **1980**, *72,* 5639.

(23) Pople, J. A.; Head-Gordon, M.; Raghavachari, K. *J. Chem. Phys.* **1987**, *87*, 5968.

(24) Hunsicker, S.; Jones, R. O. *J. Chem. Phys.* **1996**, *105*, 5048.

(25) Siegbahn, P. E. M. *J. Chem. Phys.* **1980**, *72*, 1647.

(26) Werner, H.-J.; Knowles, P. J. *J. Chem. Phys.* **1988**, *89*, 5803.

(27) Knowles P. J.; Werner, H.-J. *Chem. Phys. Lett.* **1988**, *145*, 514.

(28) Raghavachari, K.; Trucks, G. W.; Pople, J. A.; Head-Gordon, M. *Chem. Phys. Lett.* **1989**, *157*, 479.

(29) Scuseria, G. E. *Chem. Phys. Lett.* **1991**, *176*, 27.

(30) Watts, J. D.; Gauss, J.; Bartlett, R. J. *J. Chem. Phys.* **1993**, *98*, 8718.

(31) Hampel, C.; Peterson, K.; Werner, H.-J. *Chem. Phys. Lett.* **1992**, *190*, 1.

(32) Knowles, P. J.; Hampel, C.; Werner, H.-J. *J. Chem. Phys.* **1993**, *99*, 5219.

(33) Almlöf, J.; Taylor, P. R. *J. Chem. Phys.* **1987**, *86*, 4070.

(34) Almlöf, J.; Taylor, P. R. *J. Chem. Phys.* **1990**, *92*, 551.

(35) Dunning, Jr. T. H. *J. Chem. Phys.* **1989**, *90*, 1007.

(36) Kendall, R. A.; Dunning, Jr., T. H.; Harrison, R. J. *J. Chem. Phys.* **1992**, *96*, 6796.

(37) Woon, D. E.; Dunning, Jr., T. H. *J. Chem. Phys.* **1990**, *98*, 1358.

(38) Bauschlicher, Jr., C. W.; Langhoff, S. R.; Taylor, P. R. *Adv. Chem. Phys.* **1990**, *77*, 103.

(39) Lee, T. J.; Scuseria, G. E. In *Quantum Mechanical Electronic Structure Calculations with Chemical Accuracy*; Langhoff, S. R., Ed.; Kluwer: Dordrecht, 1995; p 47.

(40) Cai, Z.-L.; Martin, J. M. L.; François, J. P.; Gijbels, R. *Chem. Phys. Lett.* **1996**, *252*, 398.

(41) Cai, Z.-L.; François, J. P. *Chem. Phys.* **1998**, *234*, 59.

(42) Werner, H.-J.; Knowles, P. J. *J. Chem. Phys.* **1985**, *82*, 5053.

(43) Knowles, P. J.; Werner, H.-J. *Chem. Phys. Lett.* **1985**, *115*, 259.

(44) MOLPRO 96 is a package of ab initio programs written by Werner, H.-J.; Knowles, P. J., with contribution from Almlöf, J.; Amos, A. D.; Berning, A.; Deegan, M. J. O.; Eckert, F.; Elbert, S. T.; Hampel, C.; Lindh, R.; Meyer, W.; Nicklass, A.; Peterson, K.; Pitzer, P.; Stone, A. J.; Taylor, P. R.; Mura, M. E.; Pulay, P.; Schütz, M.; Stoll, H.; Thorsteinsson, T.; Cooper, D. L.

(45) Gaussian 94 Revision B.1 is a package written by Frisch, M. J.; Trucks, G. W.; Schlegel, H. B.; Gill, P. M. W.; Johnson, B. G.; Robb, M. A.; Cheeseman, J. R.; Keith, T.; Petersson, G. A.; Montgomery, J. A.; Raghavachari, K.; Al-Laham, M. A.; Zakrzewski, V. G.; Ortiz, J. V.; Foresman, J. B.; Cioslowski, J.; Stefanov, B. B.; Nanayakkara, A.; Challacombe, M.; Peng, C. Y.; Ayala, P. Y.; Chen, W.; Wong, M. W.; Andres, J. L.; Replogle, E. S.; Gomperts, R.; Martin, R. L.; Fox, D. J.; Binkley, J. S.; Defrees, D. J.; Baker, J.; Stewart, J. J. P.; Head-Gordon, M.; Gonzalez, C.; Pople, J. A. (Gaussian Inc. Pittsburgh, 1995).

(46) Martin, J. M. L.; Taylor, P. R. *Chem. Phys. Lett.* **1994**, *225*, 413.

(47) Martin, J. M. L. *Chem. Phys. Lett.* **1995**, *242*, 343.

(48) Andersson, K. A.; Fülscher, M. P.; Karlström, G.; Lindh, R.; Malmqvist, P.-Å.; Oslen, J.; Roos, B. O.; Sadlej, A.; Blomberg, M. R. A.; Siegbahn, P. E. M.; Kellö, V.; Noga, J.; Urban, M.; Widmark, P.-O. MOLCAS 2; University of Lund, Sweden, 1992.

(49) Peterson, K. A.; Kendall, R. A.; Dunning, Jr., T. H. *J. Chem. Phys.* **1993**, *99*, 9790.

(50) Larsson, M. *Astron. Astrophys.* **1983**, *128*, 291.

(51) Chase, Jr., M. W.; Davies, C. A.; Downey, Jr. J. R.; Frurip, D. J.; McDonald, R. A.; Syverud, A. N. *JANAF Thermochemical Tables*, 3rd ed.; American Chemical Society and the American Institute of Physics (for National Bureau of Standards): New York, 1986.

(52) Martin, J. M. L. *Chem. Phys. Lett.* **1996**, *259*, 669.

(53) Woon, D. E.; Dunning, Jr., T. H. *J. Chem. Phys.* **1993**, *99*, 1914.

(54) Cai, Z.-L.; François, J. P. *Chem. Phys. Lett.* **1998**, *282*, 29.